

# Measuring the Leptonic CP Phase in $\nu_\mu \rightarrow \nu_\mu$ Oscillations

KEIICHI KIMURA<sup>1</sup> AKIRA TAKAMURA<sup>1,2</sup>

AND

TADASHI YOSHIKAWA<sup>1</sup>

<sup>1</sup>*Department of Physics, Nagoya University, Nagoya, 464-8602, Japan*

<sup>2</sup>*Department of Mathematics, Toyota National College of Technology*

*Eisei-cho 2-1, Toyota-shi, 471-8525, Japan*

## Abstract

In  $\nu_\mu \rightarrow \nu_\mu$  oscillations, we find that the effect of the CP phase  $\delta$  becomes large in the region  $E < 2$  GeV and  $L > 2000$  km. In this region, the change of the probability in this channel reaches about 0.4 due to the CP phase effect beyond our expectation in the case of large 1-3 mixing angle. Furthermore, the CP phase effect have almost same sign over the region  $E > 0.5$  GeV so that one may find the signal of CP violation by measuring the total rate only. As an example, we use an experimental setup and demonstrate that the allowed region is limited to one by combined analysis of  $\nu_e$  and  $\nu_\mu$  events although there remain three allowed regions by the analysis of  $\nu_e$  events alone.

## 1 Introduction

The measurement of the leptonic CP phase is one of the most important aims in elementary particle physics. A lot of investigations for this possibility have been performed, see [1, 2, 3, 4, 5, 6, 7, 8] and the references therein. In most of these investigations,  $\nu_e \rightarrow \nu_\mu$  or  $\nu_\mu \rightarrow \nu_e$  oscillations (so-called golden channel [2]) are used for the measurement of  $\delta$  and  $\nu_e \rightarrow \nu_\tau$  oscillations (silver channel [6]) are also used partly. However, there are also  $\nu_\mu \rightarrow \nu_\mu$  oscillations as another channel observed in long baseline experiments. The measurement of  $\delta$  in this channel have been considered to be difficult because the probability  $P_{\mu\mu}$  depends almost only on the  $\cos\delta$  term and the CP dependence disappears in the case of  $\delta = 90^\circ$  and  $270^\circ$ . However, some recent papers discuss the possibility of solving the parameter ambiguity by using this channel [9, 10]. In these analysis, the CP dependence becomes small and the confirmation of  $\delta$  seems to be difficult in actual experiments. However, if the CP dependence becomes large in this channel, this analysis is very useful, interesting and cost-effective because the probability of this channel can be measured at the same time as  $\nu_\mu \rightarrow \nu_e$  probability without any extra apparatus and we can obtain another information on the CP phase in superbeam experiments. In quark sector, the CP violation was discovered in K physics, but the determination of the CP phase cannot be performed by the increase of the data in K physics and needed the B-factory experiments [11]. The measurement of the CP phase in two different channels is considered to be very important also for the lepton sector. We obtain the information with a different nature by using different channels. Furthermore, this opens the window for a verification of the unitarity in three generation and exploration of new physics.

In the previous paper, we introduced a new index of the leptonic CP phase dependence  $I_{\text{CP}}$  and investigated how the information of  $\delta$  can be obtained through the channel of  $\nu_\mu \rightarrow \nu_e$  oscillation [12]. In this letter, we use  $I_{\text{CP}}$  for the channel of  $\nu_\mu \rightarrow \nu_\mu$  oscillation and explore the region in  $E$ - $L$  plane where the CP dependence becomes large. We consider one baseline in this region and investigate the contribution of the CP phase to  $\nu_\mu \rightarrow \nu_\mu$  oscillations in detail. Finally, we simulate both  $\nu_\mu$  and  $\nu_e$  events by using an experimental setup and compare the analysis of  $\nu_e$  events alone with the combined analysis of  $\nu_\mu$  and  $\nu_e$  events.

## 2 Large CP Dependence in $\nu_\mu \rightarrow \nu_\mu$ Oscillations

At first, we write the Hamiltonian in matter [13] as

$$H = O_{23}\Gamma H'\Gamma^\dagger O_{23}^T \quad (1)$$

by factoring out  $\theta_{23}$  and  $\delta$ , where  $O_{23}$  is the rotation matrix in the 2-3 generations and  $\Gamma$  is the phase matrix defined by  $\Gamma = \text{diag}(1, 1, e^{i\delta})$ . The reduced Hamiltonian  $H'$  is given by

$$H' = O_{13}O_{12}\text{diag}(0, \Delta_{21}, \Delta_{31})O_{12}^T O_{13}^T + \text{diag}(a, 0, 0), \quad (2)$$

where  $\Delta_{ij} = \Delta m_{ij}^2/(2E) = (m_i^2 - m_j^2)/(2E)$ ,  $a = \sqrt{2}G_F N_e \simeq 7.56 \times 10^{-5} \cdot \rho Y_e$ ,  $G_F$  is the Fermi constant,  $N_e$  is the electron number density,  $Y_e$  is the electron fraction,  $E$  is neutrino energy and  $m_i$  is the mass of  $\nu_i$ . The oscillation probability for  $\nu_\mu \rightarrow \nu_\mu$  is proportional to the  $\cos \delta$  and  $\cos 2\delta$  in constant matter profile [14] and can be expressed as

$$P_{\mu\mu} = A \cos \delta + C + D \cos 2\delta. \quad (3)$$

Here,  $A$ ,  $C$  and  $D$  are determined by parameters other than  $\delta$  and are calculated by

$$A = 4\text{Re}[(S'_{\mu\mu}c_{23}^2 + S'_{\tau\tau}s_{23}^2)^* S'_{\mu\tau}]c_{23}s_{23}, \quad (4)$$

$$C = |S'_{\mu\mu}|^2 c_{23}^4 + |S'_{\tau\tau}|^2 s_{23}^4 \quad (5)$$

$$+ 2(|S'_{\mu\tau}|^2 + \text{Re}[S'_{\mu\mu}^* S'_{\tau\tau}])c_{23}^2 s_{23}^2, \quad (6)$$

$$D = 2|S'_{\mu\tau}|^2 c_{23}^2 s_{23}^2, \quad (7)$$

where  $S'_{\alpha\beta} = [\exp(-iH'L)]_{\alpha\beta}$ . In the case of symmetric density profile and  $\theta_{23} = 45^\circ$ , the coefficient  $A$  coincides with  $A_{e\mu}$ , which is the coefficient of  $\cos \delta$  in the  $\nu_\mu \rightarrow \nu_e$  oscillation probability, except for the sign [15]. Namely,  $A$  is simplified as

$$A = -A_{e\mu} = -\text{Re}[S'_{\mu e}^* S'_{\tau e}]. \quad (8)$$

If we notice the small parameters,  $\alpha = \Delta_{21}/\Delta_{31}$  and  $\sin \theta_{13} = s_{13}$  and count the order of coefficients, we obtain  $A = O(\alpha s_{13})$ ,  $C = O(1)$  and  $D = O(\alpha^2 s_{13}^2)$ . Therefore, this leads to the relation  $D \ll A \ll C$  and we can safely neglect the term including  $D$  [15].

Next, we introduce  $I_{\text{CP}}$  following [12]. Suppose that  $P_{\text{max}}$  and  $P_{\text{min}}$  as the maximal and minimal values when  $\delta$  changes from  $0^\circ$  to  $360^\circ$ . Then,  $I_{\text{CP}}$  is defined by

$$I_{\text{CP}} = \frac{P_{\text{max}} - P_{\text{min}}}{P_{\text{max}} + P_{\text{min}}} \quad (9)$$

also in  $\nu_\mu \rightarrow \nu_\mu$  oscillation. As the coefficient  $D$  can be neglected,  $P_{\mu\mu}$  is approximated by  $P_{\mu\mu} \simeq A \cos \delta + C$ .  $P_{\text{max}}$  and  $P_{\text{min}}$  correspond to the two end points. Namely, the maximal and minimal values are given by  $P_{\mu\mu} \simeq A + C$  or  $-A + C$  corresponding to  $\delta = 0^\circ$  or  $180^\circ$ . So, we obtain

$$I_{\text{CP}} \simeq \frac{|A|}{C}. \quad (10)$$

Next, let us present the region with large  $I_{\text{CP}}$  in  $E$ - $L$  plane. In order to exclude the region with large  $I_{\text{CP}}$  due to the small denominator, we also show the region with large  $|A|$ , which is the numerator of  $I_{\text{CP}}$ . In fig.1, we assume  $\sin^2 2\theta_{13} = 0.16$ , which is near the upper bound of the CHOOZ experiment [16], and can be measured in the next generation reactor experiments [17, 18]. If  $\theta_{13}$  will be determined by this method without ambiguity, we can take a large step for the measurement of  $\delta$  [19]. We use the best-fit values  $\Delta m_{21}^2 = 7.9 \times 10^{-5} \text{eV}^2$ ,  $\sin^2 \theta_{12} = 0.31$ ,  $\Delta m_{31}^2 = 2.2 \times 10^{-3} \text{eV}^2$  and  $\sin^2 \theta_{23} = 0.50$  [20] for other parameters. We calculate by using the matter density  $\rho = 3.3 \text{g/cm}^3$ . In fig.1, black color shows the region with  $I_{\text{CP}} > 30\%$  and  $|A| > 20\%$  respectively in left and right figures. Comparing the two figures, we can see that the region with large  $I_{\text{CP}}$  does not overlap that with large  $|A|$  above 2 GeV. This means that the region of large  $I_{\text{CP}}$  above 2 GeV just indicates the region where the denominator is small. On the other hand, both regions overlap over wide region below 2 GeV. We found from fig.1 that the CP dependence in  $\nu_\mu \rightarrow \nu_\mu$  oscillations becomes large in the region  $E < 2$  GeV and  $L > 2000$  km. We choose a baseline of  $L = 3000$  km as an example in this region and investigate the behavior of  $A$  and  $P_{\mu\mu}$  in detail. See ref. [21] about other baselines.

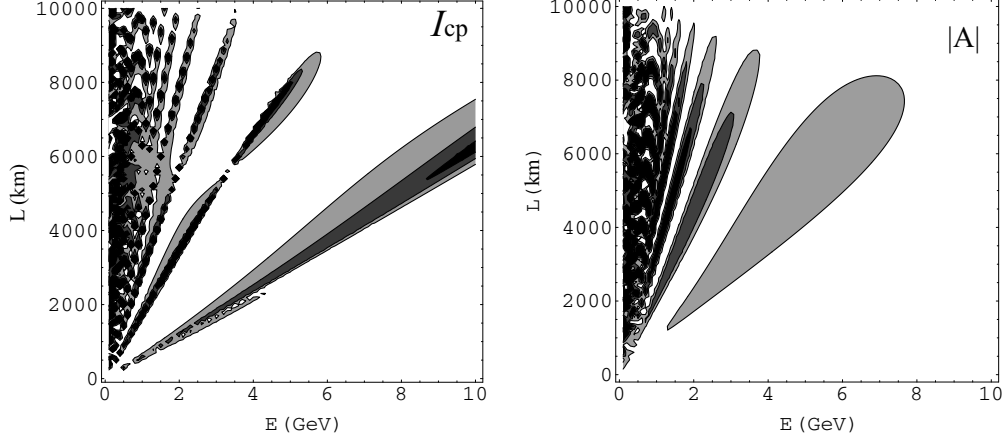


Fig.1. Region with large  $I_{CP}$  (Left) and large  $|A|$  (Right). The region with black color has a value larger than 30% for  $I_{CP}$  and 20% for  $|A|$ . Left and right panels show the region for  $I_{CP}$  and  $|A|$ .

In fig.2, we calculate the energy dependence of  $A$  and  $P_{\mu\mu}$  at  $L = 3000$  km by using the exact expressions (8) and (3).  $P_{\mu\mu}$  is plotted in the energy region  $E = 0.4$ - $1.2$  GeV for the correspondence to the simulation of the number of events.

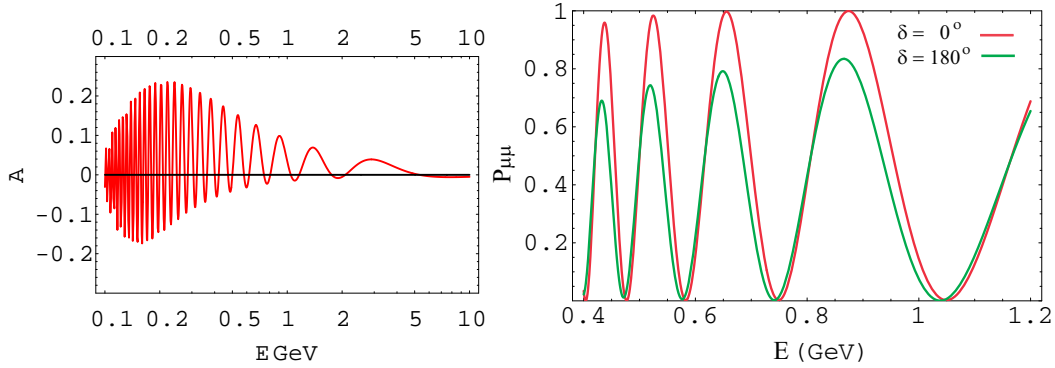


Fig.2. Energy dependence of  $A$  and  $P_{\mu\mu}$ . Left figure shows the magnitude of  $A$ . In the right figure, the two lines show the oscillation probabilities with  $\delta = 0^\circ$  and  $180^\circ$ , respectively.

In fig.2(left), one can see that the maximal value of  $A$  reaches almost about 0.2 and the probabilities for  $\delta = 0^\circ$  and  $180^\circ$  have a difference about 0.4 around  $E \simeq 0.2$  GeV. In addition, the coefficient  $A$  is almost positive over the region  $E > 0.5$  GeV and we expect a large CP dependence in total  $\nu_\mu$  events accumulated in this region. If the coefficient  $A$  oscillates between positive and negative values, they contribute destructively and the CP phase effect becomes small in the total events. Therefore, the fact of  $A \geq 0$  in whole region of  $E > 0.5$  GeV is very useful for the measurement of the CP phase effect. This is one of the important points of this paper.

In fig.2 (right), we can see that the probabilities in the case of  $\delta = 0^\circ$  and  $\delta = 180^\circ$  have a difference about 0.3 in the energy region  $E = 0.4$ - $0.6$  GeV. This can be understood by the magnitude of  $A$  for the corresponding energy region in fig.2 (left). Up to now, the CP dependence in  $\nu_\mu \rightarrow \nu_\mu$  oscillations is neglected in a lot of works. Probably, one reason for this is that  $P_{\mu\mu}$  depends only on  $\cos\delta$  and the CP dependence disappears in the case of  $\delta = 90^\circ$  and  $270^\circ$ . Another reason is that the analysis satisfying the conditions  $E < 2$  GeV and  $L > 2000$  km is limited. In this letter, we found that there is a possibility for measuring  $\delta$  by using the channel of  $\nu_\mu \rightarrow \nu_\mu$  oscillation under the above conditions.

In order to understand the features in fig.2, let us consider the approximate formula of  $A$ . The expression for (8) is given by

$$A \simeq -\frac{4\Delta_{21}\Delta_{31}s_{12}c_{12}s_{13}c_{13}}{\Delta_\ell\Delta_h}\sin\frac{\Delta_\ell L}{2}\sin\frac{\Delta_h L}{2}\cos\frac{\Delta_{32}L}{2}, \quad (11)$$

where  $\Delta_h = \Delta m_h^2/(2E)$ ,  $\Delta_\ell = \Delta m_\ell^2/(2E)$  and  $\Delta m_h^2$  ( $\Delta m_\ell^2$ ) is mass squared difference in matter [22, 2, 15]. The concrete expression for  $\Delta_h$  is given by

$$\Delta_h = \sqrt{(\Delta_{31} \cos 2\theta_{13} - a)^2 + \Delta_{31} \sin^2 2\theta_{13}} \simeq \Delta_{31} - a. \quad (12)$$

The second equality approximately holds in the case of  $\sin \theta_{13} \ll 1$ . We also obtain  $\Delta_\ell$  by the replacements,  $\Delta_h \rightarrow \Delta_\ell$ ,  $\Delta_{31} \rightarrow \Delta_{21}$  and  $\theta_{13} \rightarrow \theta_{12}$  as

$$\Delta_\ell = \sqrt{(\Delta_{21} \cos 2\theta_{12} - a)^2 + \Delta_{21} \sin^2 2\theta_{12}} \simeq a. \quad (13)$$

The second equality approximately holds in the case of  $a \gg \Delta_{21} = \Delta m_{21}^2/2E$ . If we substitute  $\rho = 3.3\text{g/cm}^3$  and the electron fraction in the mantle  $Y_e = 0.494$ , we obtain  $a = 1.2 \times 10^{-4}$  and  $\Delta_\ell \simeq a$  becomes a good approximation for  $E \gg \Delta m_{21}^2/2a = 0.3 \text{ GeV}$ . Furthermore, at the baseline  $L = 3000 \text{ km}$ , we obtain

$$\sin \frac{\Delta_\ell L}{2} \simeq \sin \frac{aL}{2} \simeq 0.8. \quad (14)$$

Therefore, the last two terms included in (11) are rewritten as

$$\begin{aligned} 2 \sin \frac{\Delta_h L}{2} \cos \frac{\Delta_{32} L}{2} &\simeq 2 \sin \frac{(\Delta_{31} - a)L}{2} \cos \frac{\Delta_{31} L}{2} \\ &= \left\{ \sin \left( \Delta_{31} L - \frac{aL}{2} \right) - \sin \frac{aL}{2} \right\}, \end{aligned} \quad (15)$$

and they oscillate within the limits given by

$$-1 - \sin \frac{aL}{2} < 2 \sin \frac{\Delta_h L}{2} \cos \frac{\Delta_{32} L}{2} < 1 - \sin \frac{aL}{2}. \quad (16)$$

Note that this takes value from  $-2$  to  $0$ , namely always negative, if  $\sin \frac{aL}{2} \sim 1$ . As a result, we can roughly estimate  $A$  as

$$0 \leq A \leq \frac{0.4\Delta_{21}\Delta_{31}}{a(\Delta_{31} - a)} \simeq \frac{0.4\Delta_{21}}{a} \sim \frac{0.13}{E} \quad (17)$$

in  $E > 0.5 \text{ GeV}$  and can understand the reason for being always positive in fig.2 (left). We can also explain that the coefficient  $A$  is inverse proportional to the energy and decreases according to the increase of the energy. Furthermore, we find the position of the peak of  $A$  as  $2 \cdot 1.27(\Delta m_{31}^2 - aE)L/E = (2n + 3/2)\pi$  ( $n = 0, 1, 2, \dots$ ) from (15). If we substitute  $\Delta m_{31}^2 = 2.2 \cdot 10^{-3} \text{eV}^2$  and  $L = 3000 \text{ km}$ , we obtain the peak energy as  $E = 1.27\Delta m_{31}^2 L / (2n + 7/4)\pi = 5.3 / (2n + 7/4)$ . The peak with highest energy is obtained at  $E = 3 \text{ GeV}$  by substituting  $n = 0$ . Thus,  $A$  has large value and is almost positive over the energy region about  $E = 0.5\text{-}5 \text{ GeV}$ . Here, we also note the  $\theta_{13}$  dependence of  $A$ . As seen from (11), the CP phase effect becomes small according to the decrease of  $\theta_{13}$ .

Finally, let us briefly comment on the value of  $I_{CP}$  for  $\nu_\mu \rightarrow \nu_e$  oscillations as preparation of combined analysis using both  $\nu_\mu$  and  $\nu_e$  events in the next section. We have investigated how  $I_{CP}$  for  $\nu_\mu \rightarrow \nu_e$  oscillations changes according to the values of  $E$  and  $L$  in the previous paper [12]. See fig.1 (left) in ref.[12]. As a result, we found that the value of  $I_{CP}$  takes nearly maximal value also in the region  $E < 2 \text{ GeV}$  and  $L > 2000 \text{ km}$  for  $\nu_\mu \rightarrow \nu_e$  oscillations. This means that the absolute values of  $S'_{\tau e}$  and  $S'_{\mu e}$  have an same order, namely the solar term is as large as the atmospheric term in this region. In the large  $I_{CP}$  region, we can expect that the  $\delta$  dependence of the number of events also becomes large.

### 3 Estimation of Signal from Leptonic CP Phase

Next, let us consider an experimental setup and estimate the CP phase effect. In order to utilize the  $\delta$  dependence of  $\nu_\mu$  events in addition to that of  $\nu_e$  events, we would like to choose the experimental setup, which satisfies the condition  $E \simeq 0.5\text{-}2$  GeV and  $L > 2000\text{km}$  obtained in sec.2. As such an example, we consider the 4MW beam and the 1Mt water Cherenkov detector, which are the same used in the JPARC-HyperKamiokande experiment [23], but we take  $L = 3000$  km as the baseline length. In fig.3, we numerically calculate the signal of  $\nu_\mu$  disappearance (left) and  $\nu_e$  appearance (right), namely the total number of events distinct from the background noise, obtained in the above experimental setup within the energy range  $E = 0.4\text{-}1.2$  when the CP phase  $\delta$  changes from  $0^\circ$  to  $360^\circ$ . We assume here only the neutrino beam data acquisition for two years and we use the same parameters as in fig.2. We also give the statistical error within the  $2\text{-}\sigma$  level in fig.3. We use the globes software to perform the numerical calculation [24, 23].

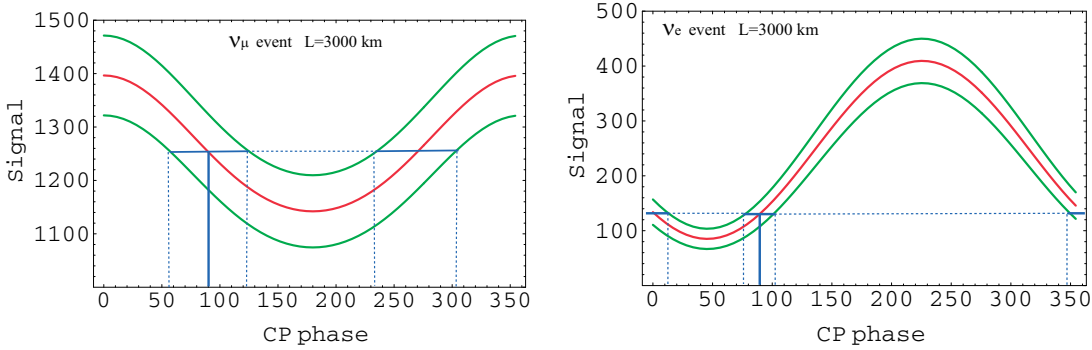


Fig.3. CP dependence of  $\nu_\mu$  disappearance and  $\nu_e$  appearance signal. Left and right panels show the  $\nu_\mu$  and  $\nu_e$  signal. The statistical error is also shown within the  $2\text{-}\sigma$  level.

Fig.3 (left) shows that the number of  $\nu_\mu$  events becomes maximal around  $\delta = 0^\circ$  and minimal around  $\delta = 180^\circ$  as expected from the oscillation probability in fig.2 (right). We obtain the number of events between these values in the case of  $\delta = 90^\circ$  or  $270^\circ$ . We find that the number of  $\nu_\mu$  events changes about 250 due to the CP phase effect. On the other hand, fig.3 (right) shows that the number of  $\nu_e$  events becomes maximal around  $\delta = 45^\circ$  and minimal around  $\delta = 225^\circ$ . We also find that the number of  $\nu_e$  events changes about 300 due to the CP phase effect.

Next, let us explain the merit of the combined analysis of the total events in these two channels compared with the analysis of  $\nu_e$  events alone. We assume  $\delta = 90^\circ$  as the true value of the CP phase. Then, about 120  $\nu_e$  events are expected and we obtain the information on the value of  $\delta$  as  $0^\circ \leq \delta \leq 15^\circ$  or  $75^\circ \leq \delta \leq 105^\circ$  or  $350^\circ \leq \delta \leq 360^\circ$ . If the standard model is correct and the unitarity holds, about 1260  $\nu_\mu$  events are expected. From this result, we obtain the information  $60^\circ \leq \delta \leq 130^\circ$  or  $235^\circ \leq \delta \leq 300^\circ$ . If we combine the above information obtained by the two different channels, the extent of  $\delta$  is limited to  $75^\circ \leq \delta \leq 105^\circ$ . Thus, there remain three allowed regions in the analysis of  $\nu_e$  events alone. On the other hand, one allowed region is chosen in the combined analysis of two channels. Furthermore, if the number of  $\nu_\mu$  events are largely different from 1260, this is considered to be the signal of some new physics beyond the standard model.

In fig.4, we also show the simultaneous fit of  $s_{13}$  and  $\delta$  by assuming the true values,  $\sin^2 2\theta_{13} = 0.16$  and  $\delta = 90^\circ$ . Other parameters are the same as the values used in fig.3. We define  $\Delta\chi_{\nu_e}^2$  and  $\Delta\chi_{\nu_e+\nu_\mu}^2$  as

$$\Delta\chi_{\nu_e}^2 = \frac{(N_{\nu_e} - N_{\nu_e}^{true})^2}{N_{\nu_e}^{true}} \quad (18)$$

$$\Delta\chi_{\nu_e+\nu_\mu}^2 = \frac{(N_{\nu_e} - N_{\nu_e}^{true})^2}{N_{\nu_e}^{true}} + \frac{(N_{\nu_\mu} - N_{\nu_\mu}^{true})^2}{N_{\nu_\mu}^{true}}, \quad (19)$$

where  $N_{\nu_i}$  and  $N_{\nu_i}^{true}$  represent the number of  $\nu_i$  events calculated by using the test values and true values respectively. In the left panel, the contours for 1, 2 and 3- $\sigma$  C.L. with  $\Delta\chi_{\nu_e}^2 = 2.3, 6.18$  and 11.83 are

drawn as solid, dotted and dashed lines. In the same way, the contours for  $\Delta\chi^2_{\nu_e+\nu_\mu}$  are drawn in the right panel. In our analysis, only the statistical error is included for the simplicity. Here, we also use the globes software to perform the numerical calculation [24, 23].

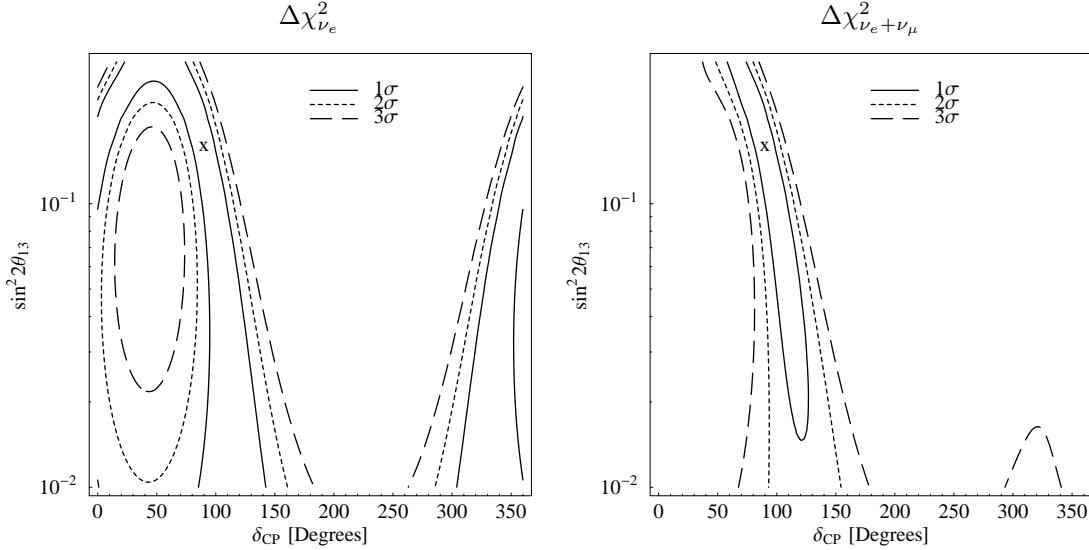


Fig.4. Simultaneous fit of  $s_{13}$  and  $\delta$  by assuming the true values,  $\sin^2 2\theta_{13} = 0.16$  and  $\delta = 90^\circ$ . Left and right panels are drawn assuming the measurement of  $\nu_e$  events alone and both  $\nu_\mu$  and  $\nu_e$  events. The true values are represented by x in these figures. The statistical error is also shown as solid, dotted and dashed contours for 1,2 and 3- $\sigma$  ( $\Delta\chi^2 = 2.3, 6.18$  and  $11.83$ ) respectively.

Comparing the left and right panels, we also found that some allowed regions are excluded by the additional measurement of  $\nu_\mu$  events. Another notable point is that the value of  $\Delta\chi^2$  seems to remain unchanged even in the case for small  $\sin^2 2\theta_{13}$ . We can understand this result by the following reason. The appearance probability for  $\nu_\mu$  to  $\nu_e$  transition does not change largely because  $\theta_{13}$  independent term (the solar term) is comparatively large in such low energy region and is not so affected by the value of  $\theta_{13}$ . Therefore, the value of  $\Delta\chi^2$  does not change largely by the decrease of  $\theta_{13}$ .

Here, let us emphasize again on the importance of the simultaneous utilization of the  $\nu_\mu \rightarrow \nu_\mu$  and  $\nu_\mu \rightarrow \nu_e$  oscillations. This provides the variable possibility for the measurement of the CP phase in future experiments. We need to investigate further, including the parameter ambiguity problem [3, 4, 5], background, systematic error and spectral dependence [21]. We also comment on the BNL-HS experiment [25]. In this experiment,  $L = 2540$  km is taken as the baseline length and the peak energy of the neutrino beam is planned about  $E = 1-2$  GeV. This setup satisfy the conditions  $E < 2$  GeV and  $L > 2000$ km derived in this letter and is similar to our test experimental setup, so we expect the observation of the CP phase effect also in the BNL-HS experiment in the case of large  $\theta_{13}$ .

## 4 Summary and Discussion

In summary, we have investigated the possibility for the measurement of the CP phase  $\delta$  by using  $\nu_\mu \rightarrow \nu_\mu$  oscillations. The measurement of  $\delta$  in this channel have been considered to be difficult because the probability  $P_{\mu\mu}$  depends only on the  $\cos\delta$  term and the CP dependence disappears in the case of  $\delta = 90^\circ$  and  $270^\circ$ . We have used  $I_{CP}$  and  $|A|$  (numerator of  $I_{CP}$ ) for this channel and have found the CP phase effect becomes large in the region  $L > 2000$ km and  $E < 2$  GeV beyond our expectation. As a result, we have shown that the difference between the probabilities for  $\delta = 0^\circ$  and  $180^\circ$  reaches about 0.4 in the case of large  $\theta_{13}$ . In addition,  $A$  is almost positive definite over the region  $E > 0.5$  GeV and we expect a large CP dependence in total  $\nu_\mu$  events accumulated in this region. As an example, we have used an experimental setup and have demonstrated that the allowed region is limited to one by combined analysis of  $\nu_e$  and  $\nu_\mu$  events although there remain three allowed regions by the analysis of  $\nu_e$  events alone. Furthermore, this channel opens the window for a verification of the unitarity in three generation and exploration of new physics beyond the standard model.

## Acknowledgement

We would like to thank Prof. Wilfried Wunderlich (Tokai university) for helpful comments and advice on English expressions.

## References

- [1] J. Arafune, M. Koike and J. Sato, Phys. Rev. **D56** (1997) 3093; Erratum-ibid. D60 (1999) 119905.
- [2] A. Cervera *et al.*, Nucl. Phys. **B579** (2000) 17.
- [3] J. Burguet-Castell *et al.*, Nucl. Phys. **B608** (2001) 301.
- [4] H. Minakata and H. Nunokawa, JHEP **0110** (2001) 001.
- [5] V. Barger, D. Marfatia and K. Whisnant, Phys. Rev. **D65** (2002) 073023.
- [6] A. Donini, D. Meloni and P. Migliozi, Nucl. Phys. **B646** (2002) 321.
- [7] H. Minakata, hep-ph/0402197; M. Ishitsuka *et. al.*, Phys. Rev. **D72** (2005) 033003.
- [8] P. Huber, M. Lindner and W. Winter, JHEP **0505** (2005) 020.
- [9] K. Whisnant, J. M. Yang, and B-L. Young, Phys. Rev. **D67** (2003) 013004.
- [10] R. Gandhi, P. Ghoshal, S. Goswami, P. Mehta, and S U. Sankar, Phys.Rev. **D73** (2006) 053001.
- [11] A. B. Carter and A. I. Sanda, Phys. Rev. **D23** (1981) 1567; I. I. Bigi and A. I. Sanda, Nucl. Phys. **B193** (1981) 85; Phys. Rev. **D29** (1984) 1393.
- [12] K. Kimura, A. Takamura and T. Yoshikawa, Phys. Lett. **B640** (2006) 32.
- [13] Z. Maki, M. Nakagawa and S. Sakata, Prog. Theor. Phys. **28** (1962) 870.
- [14] K. Kimura, A. Takamura and H. Yokomakura, Phys. Lett. **B537** (2002) 86; Phys. Rev. **D66** (2002) 073005; J. Phys. **G29** (2003) 1839, Phys. Lett. **B544** (2002) 286.
- [15] A. Takamura, K. Kimura and H. Yokomakura, Phys. Lett. **B595** (2004) 414; Phys. Lett. **B600** (2004) 91; JHEP **0601** (2006) 053.
- [16] CHOOZ Collaboration, M. Apollonio *et al.*, Phys. Lett. **B466** (1999) 415.
- [17] The Double-CHOOZ collaboration, F. Ardellier *et al.*, hep-ex/0405302.
- [18] The KASKA collaboration, F. Suekane, hep-ex/0407016.
- [19] H. Minakata, H. Sugiyama, O. Yasuda, K. Inoue and F. Suekane, Phys. Rev. **D68** (2003) 033017; Erratum-ibid. **D70** (2004) 059901.
- [20] T. Schwetz, Acta Phys. Polon. **B36** (2005) 3203.
- [21] K. Kimura, A. Takamura and T. Yoshikawa, work in progress.
- [22] M. Freund, Phys. Rev. **D64** (2001) 053003.
- [23] Y. Itow *et. al.*, hep-ex/0106019.
- [24] P. Huber, M. Lindner and W. Winter, Nucl. Phys. **B645** (2002) 3; Comput. Phys. Commun. **167** (2005) 195.
- [25] M.V. Diwan *et al.*, Phys. Rev. **D68** (2003) 012002.